PROGRESS IN APPLIED SCIENCE AND TECHNOLOGY
Faculty of Science and Technology
Rajamangala University of Technology Thanyaburi
Vol.11 No.1 (2021): xx–xx
ISSN (Print): 2730-3012
ISSN (Online): 2730-3020
https://ph02.tci-thaijo.org/index.php/past

Received 04th October 2020,
Revised 10th January 2021,
Accepted 19th February 2021

DOI: 10.14456/x0xx00000x

Theoretical investigation of NO_2 adsorption on C–, Si–, and Ge–doped boron nitride nanomaterials

Wandee Rakrai[1], Chanukorn Tabtimsai[1], and Banchob Wanno[2*]
[1] *Department of Chemistry, Computational Chemistry Center for Nanotechnology (CCCN), Faculty of Science and Technology, Rajabhat Maha Sarakham University, Maha Sarakham, 44000, Thailand*
[2] *Center of Excellence for Innovation in Chemistry (PERCH–CIC) and Supramolecular Chemistry Research Unit, Department of Chemistry, Faculty of Science, Mahasarakham University, Maha Sarakham, 44150, Thailand*
*E–mail: banchobw@gmail.com

Abstract

The adsorption abilities, structural and electronic properties of nitrogen dioxide (NO_2) molecule adsorbed on pristine, and C–, Si–, and Ge–doped boron nitride nanosheets (BNNS) and nanotubes (BNNT) were investigated using the density functional theory method. The binding energies of doping reveal that the C atom doping exhibits the strongest binding ability with both BNNS and BNNT. In addition, the NO_2 molecule weakly interacts with the pristine BNNS and BNNT, whereas it has a strong adsorption ability with C–, Si–, and Ge–doped BNNSs and BNNTs. The electronic properties such as the energy gap and partial charge transfer of all atomic doped–BNNSs and BNNTs are significantly modified after NO_2 adsorptions. Thus, the C–, Si–, and Ge–doped BNNSs and BNNTs can be used as NO_2 gas storage and sensing.

Keywords: Adsorption, Boron nitride, DFT, Nanosheet, Nanotube, Nitrogen dioxide

1. Introduction

Boron nitride (BN) nanomaterials included nanotubes and nanosheets are chemical compound, consisting of equal numbers of boron (B) and nitrogen (N) atoms, which are not found in nature and is therefore produced synthetically. One–dimensional (1D) boron nitride nanotube (BNNT) was successfully synthesized in 1995 (1) and two–dimensional (2D) hexagonal boron nitride sheet (BNNS) was peeled off from a boron nitride crystal in 2005 (2). These nanomaterials are electrically insulator with a wide band gap, high thermal conductivity and interesting magnetic features (3). These properties cause that the boron nitride nanomaterials display great potential in many fields, such as nanodevices especially the chemical sensors. However, it was found that the modified BN is more sensitive sensing than that of pristine BN, therefore the defects in BN behave some interesting characteristics. In the process of preparations or modifications, various types of defects on BN can be formed, such as adatoms (4), vacancies or doping (5). The atom (AT) doped BNNTs and BNNSs further enlarge the application in gas chemical sensor, such as NO (6, 7), CO (7), O_2 (8), H_2 (9), NH_3 (10), SO_2 (11-13) and NO_2 (13).

Nitrogen dioxide (NO_2) is one of the toxic gases with pungent smell. It can be produced during combustion in factories and thermal power plants (14). The NO_2 gas displays highly toxic to nervous system and respiratory organs of human, consequently the detection of NO_2 plays a significant role, therefore the sensitive sensor design for NO_2 detection is essential (15, 16).

In the present work, group IV atoms (C, Si, Ge) have been selected for doping due to they have nearly the same atomic radius of B and N atoms and place between group III of B and group V of N. The geometrical structures, adsorption energies, and electronic properties of NO_2 adsorption on the pristine and AT–doped BNNSs and BNNTs have been investigated.

2. Computational details

The adsorptions of NO_2 on pristine BNNS, pristine (5,5) armchair BNNT and their doping with C, Si, or Ge atom were investigated in terms of geometric and electronic properties in which both ends of all nanomaterials were saturated by hydrogen atoms to avoid the boundary effects. Then the doping of C, Si, or Ge atom onto the BNNS and BNNT was modeled so that one of boron or nitrogen atom at the

middle site of the BNNS and BNNT was replaced by the C, Si, or Ge atom. In this work, replacing of B or N atom of the BNNS and BNNT with C, Si, or Ge atom was referred to be the B (C_B–BNNS, Si_B–BNNS, Ge_B–BNNS, C_B–BNNT, Si_B–BNNT, Ge_B–BNNT) or N (C_N–BNNS, Si_N–BNNS, Ge_N–BNNS, C_N–BNNT, Si_N–BNNT, Ge_N–BNNT) sites, respectively. The adsorbed NO_2 gas was set by placing this molecule over the C, Si, or Ge atom. All calculations were performed using the GAUSSIAN 09 software package (17) at the DFT level with the Lee–Yang–Parr correlation functional (B3LYP) (18-20) and the intensive Los Alamos LanL2DZ split–valence basis set (21-23). The intensive B3LYP/LanL2DZ theoretical method was used because this method was successfully utilized for many works (6, 8, 10, 24-26).

Electronic properties, including the highest occupied molecular orbital (HOMO), the lowest unoccupied molecular orbital (LUMO), the HOMO and LUMO energy gap (E_g), and the partial charge transfer (PCT) upon pristine and C–, Si–, or Ge–doped BNNS and BNNT and their NO_2 adsorptions were also studied at the same theoretical level. The energy gap was obtained from the difference between HOMO and LUMO energies. The partial charge transfer (PCT) during gas adsorptions was defined as a change in gas charge between the adsorption processes using the natural bond orbital (NBO) analysis (27). The molecular graphics of all optimized structures were generated using the MOLEKEL 4.3 program (28). The binding energies (E_b) of C–, Si–, and Ge–doped BNNS and BNNT were calculated by the following equation:

$$E_b = E_{AT–BNNS} – (E_{BNNS} + E_{AT})$$
$$E_b = E_{AT–BNNT} – (E_{BNNT} + E_{AT})$$

where $E_{AT–BNNS}$ and $E_{AT–BNNT}$ were the total energies of C–, Si–, or Ge–doped BNNS and BNNT. The E_{BNNS} and E_{BNNT} were the total energy of monovacant BNNS and BNNT, and E_{AT} was the total energy of free C, Si, or Ge atom.

The adsorption energies (E_{ads}) of NO_2 on the pristine and C–, Si–, or Ge–doped BNNS and BNNT were determined through the following equation:

$$E_{ads} = E_{gas/\ BNNS} – (E_{BNNS} + E_{gas})$$
$$E_{ads} = E_{gas/\ BNNT} – (E_{BNNT} + E_{gas})$$

where $E_{gas/\ BNNS}$ and $E_{gas/\ BNNT}$ were the total energy of NO_2 adsorbed on pristine or C–, Si–, or Ge–doped BNNS and BNNT. The E_{BNNS} and E_{BNNT} were the total energy of the pristine or C–, Si–, or Ge–doped BNNS and BNNT, and the E_{gas} was the total energy of the isolated NO_2 molecule. A negative value of E_{ads} referred to exothermic process.

3. Results and Discussion

3.1 Geometrical structures of pristine, C–, Si–, and Ge–doped BNNSs and BNNTs and their NO_2 adsorptions

The B3LYP/LanL2DZ optimized structure of pristine BNNS is displayed in Figure 1(a). The B1–N1, B1–N2, and B1–N3 bond lengths are estimated to be 1.454, 1.452, and 1.452 Å, respectively. These data are in good agreement with the previous experiment (29) and theoretical results (30), which support the validity of this model and method. While the N1–B1–N2, N2–B1–N3, and N3–B1–N1 bond angles are estimated to be 119.7, 120.5, and 119.7°, respectively. The geometrical structure of BNNT is displayed in Figure 1(b). The B1–N1, B1–N2, and B1–N3 bond lengths are estimated to be 1.453, 1.454, and 1.454 Å, respectively, which are consistent with theoretical (31, 32) and experimental values (33). While the N1–B1–N2, N2–B1–N3, and N3–B1–N1 bond angles are estimated to be 119.2, 119.8, and 119.2°, respectively. The optimized structures of the doping of C, Si, or Ge atom onto the BNNS and BNNT are displayed in Figures 2 and 3, respectively. After replacing of B or N atom on the BNNS and BNNT with C, Si, or Ge atom, it is found that these atoms form three bonds with the nearest B or N atom. The bond lengths between the replacing atom and its neighboring three N or B atom of BNNS and BNNT are found in the range of 1.435–2.020 and 1.443–2.079 Å, respectively. Furthermore, the bond angles of all BNNS and BNNT replacing B or N atom with C, Si, or Ge atom are narrower than those of the N–B–N or B–N–B of pristine BNNS and BNNT.

The binding energies (E_b) of AT and BNNS and BNNT are displayed Table 1. The E_b values of AT–doped BNNSs and BNNTs are found in the range of –103.50 to –332.63 and –118.67 to –320.44 kcal/mol, respectively. The negative values of E_b imply that the interaction for doping atoms with BNNS and BNNT surfaces corresponds to the exothermic reaction. Furthermore, the BNNS and BNNT doping with C, Si, or Ge atom on B site shows strong interaction in comparison with the doping on N site, which is the result of having the larger E_b value. In addition, the C atom doping exhibits the strongest binding ability with both BNNS and BNNT. This may be due to atomic radius of C is nearly the same size atomic radius of B and N atoms and placed between them while atomic radius of Si and G atoms is bigger than those of atomic radius of Si and G atoms.

The optimized structures of the NO_2 adsorbed on pristine and C–, Si–, and Ge–doped BNNSs and BNNTs are displayed in Figures 4 and 5, respectively. The computed BDs between the adsorbed NO_2 and pristine BNNS and BNNT are 3.110 and 3.027 Å, respectively. The BDs between the adsorbed NO_2 and AT–doped BNNS and BNNT are found in the range of 1.581–2.296 and 2.514–2.921 Å, respectively. The short BDs confirm that the NO_2 molecule shows stronger adsorption with AT–doped BNNS and BNNT than that of pristine BNNS and BNNT.

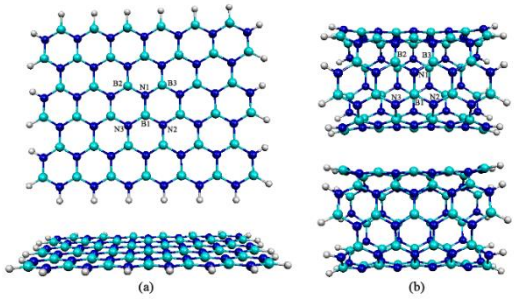

Figure 1 The B3LYP/LanL2DZ optimized structures of pristine (a) BNNS and (b) BNNT.

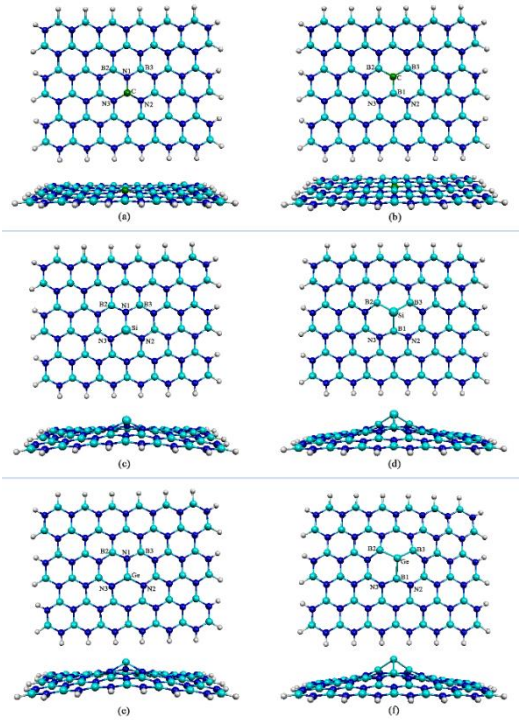

Figure 2 The B3LYP/LanL2DZ optimized structures of (a) C_B–BNNS, (b) C_N–BNNS, (c) Si_B–BNNS, (d) Si_N–BNNS, (e) Ge_B–BNNS, and (f) Ge_N–BNNS.

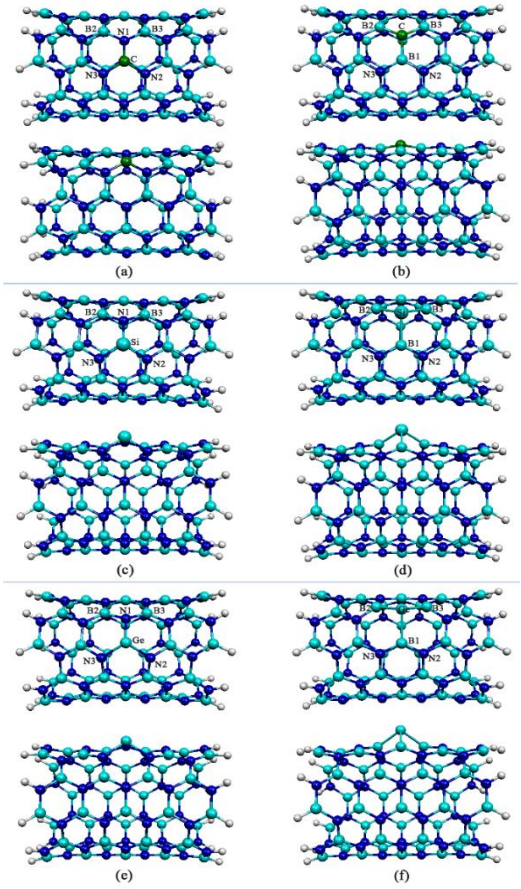

Figure 3 The B3LYP/LanL2DZ optimized structures of (a) C_B–BNNT, (b) C_N–BNNT, (c) Si_B–BNNT, (d) Si_N–BNNT, (e) Ge_B–BNNT, and (f) Ge_N–BNNT.

Table 1 The binding energies (E_b) of AT and BNNS and BNNT

Species	E_b[a]
C_B + BNNS → C_B–BNNS	–332.63
C_N + BNNS → C_N–BNNS	–295.99
Si_B + BNNS → Si_B–BNNS	–270.73
Si_N + BNNS → Si_N–BNNS	–132.88
Ge_B + BNNS → Ge_B–BNNS	–235.67
Ge_N + BNNS → Ge_N–BNNS	–103.50
C_B + BNNT → C_B–BNNT	–320.44
C_N + BNNT → C_N–BNNT	–283.54
Si_B + BNNT → Si_B–BNNT	–274.64
Si_N + BNNT → Si_N–BNNT	–146.19
Ge_B + BNNT → Ge_B–BNNT	–243.14
Ge_N + BNNT → Ge_N–BNNT	–118.67

[a] In kilocalories/mol (kcal/mol)

3.2 Adsorption energies of NO_2 molecule adsorbed on pristine, C–, Si–, and Ge–doped BNNSs and BNNTs

The adsorption energies of the NO_2 adsorbed on the pristine, C–, Si–, and Ge–doped BNNSs and BNNTs are listed in Table 3. The absorption energies of the NO_2 adsorbed on the pristine BNNS and BNNT are –2.31 and –3.52 kcal/mol, respectively. These indicate that the pristine BNNS and BNNT display a weak sensitivity to the adsorption. The adsorption abilities of the NO_2 adsorbed on the AT doped–BNNSs are in the order: NO_2/Si_B–BNNS (–78.62 kcal/mol) > NO_2/Ge_B–BNNS (–67.17 kcal/mol) > NO_2/Si_N–BNNS (–63.48 kcal/mol) > NO_2/Ge_N–BNNS (–58.51 kcal/mol) > NO_2/C_B–BNNS (–48.57 kcal/mol) > NO_2/C_N–BNNS (–33.88 kcal/mol). The adsorption abilities of the NO_2 adsorbed on the AT doped–BNNTs are in the order: NO_2/Si_B–BNNT (–69.38 kcal/mol) > NO_2/Si_N–BNNT (–64.33 kcal/mol) > NO_2/Ge_N–BNNT (–57.90 kcal/mol) > NO_2/C_B–BNNT (–52.30 kcal/mol) > NO_2/Ge_B–BNNT (–47.45 kcal/mol) > NO_2/C_N–BNNT (–46.95 kcal/mol). The results show that the NO_2 adsorptions on the C–, Si–, and Ge–doped BNNSs and BNNTs are stronger than the pristine BNNS and BNNT in which replacing of B atom of the BNNS and BNNT with Si atom displays the strongest interaction with the NO_2 molecule.

3.3 Electronic properties of pristine, C–, Si–, and Ge–doped BNNS and BNNT and their NO_2 adsorptions

For the most stable configuration of pristine, C–, Si–, and Ge–doped BNNSs and BNNTs, we examined the highest occupied molecular orbital energies (E_{HOMO}), the lowest unoccupied molecular orbital energies (E_{LUMO}), and the energy gaps (E_g). The results of which are listed in Table 2. It is found that the calculated E_g for AT–doped BNNSs and BNNTs are found in the range of 2.449–3.973 and 2.585–3.619 eV, respectively. Which are significant smaller than the E_g of pristine BNNS (5.823 eV) and BNNT (6.014). Thus, the C, Si, and Ge atom doping can induce dramatically decrease in the E_g of BNNS and BNNT, in which the chemical reactivities of C–, Si–, and Ge–doped BNNSs and BNNTs are also increased.

The electronic properties of NO_2 adsorbed on pristine, C–, Si–, and Ge–doped BNNSs and BNNTs in terms of energy gap and partial charge transfers computed at B3LYP/LanL2DZ theoretical level are listed in Table 3. When NO_2 adsorbed on the pristine BNNS and BNNT, the energy gaps of BNNS and BNNT are changed. The energy gaps of the NO_2 adsorbed on the AT doped–BNNSs and BNNTs are found in the range of 3.37–3.81 and 2.78–3.92 eV, respectively. That means, after NO_2 adsorptions, the energy gaps of all AT doped–BNNSs and BNNTs are significant changed. These results indicate that electronic properties of C–, Si–, and Ge–doped BNNSs and BNNTs are modified by NO_2 adsorptions. This means that the sensitivity of BNNS and BNNT based gas sensor for NO_2 could be improved by introducing appropriate atomic doping.

Table 2 The highest occupied molecular orbitals (E_{HOMO}), the lowest unoccupied molecular orbitals (E_{LUMO}), and energy gaps (E_g) of pristine, C–, Si–, and Ge–doped BNNS and BNNT

Species[a]	E_{HOMO}[b]	E_{LUMO}[b]	E_{gap}[b]
BNNS (1)	–6.504	–0.680	5.823
C_B–BNN_S (2)	–3.265	–0.680	2.585
C_N–BNNS (2)	–6.585	–3.891	2.694
Si_B–BNNS (2)	–6.531	–2.558	3.973
Si_N–BNNS (2)	–6.259	–3.537	2.721
Ge_B–BNNS (2)	–6.504	–3.265	3.238
Ge_N–BNNS (2)	–5.987	–3.537	2.449
BNNT (1)	–6.612	–0.599	6.014
C_B–BNNT (2)	–4.163	–0.599	3.565
C_N–BNNT (2)	–6.721	–3.946	2.776
Si_B–BNNT (2)	–6.612	–2.993	3.619
Si_N–BNNT (2)	–6.422	–3.565	2.857
Ge_B–BNNT (2)	–6.585	–3.619	2.966
Ge_N–BNNT (2)	–6.150	–3.565	2.585

[a] Spin multiplicities are in parenthesis.
[b] In eV.

N Natural bond orbital (NBO) analysis was performed to evaluate electron transfer before and after NO_2 adsorption. The partial charge transfer (PCTs) was defined as $Q_{gas/BNNS} - Q_{gas}$, and $Q_{gas/BNNT} - Q_{gas}$ for BNNS and BNNT systems, respectively, where $Q_{gas/BNNS}$ and $Q_{gas/BNNT}$ were the total charge of NO_2 adsorbed on pristine or AT doped–BNNS and BNNT, respectively, and the Qgas was the total charge of NO_2 in free case.

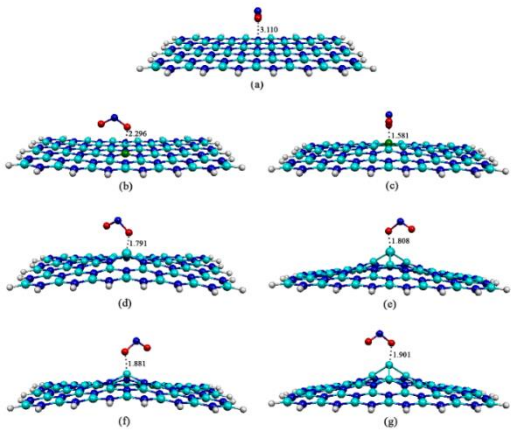

Figure 4 The B3LYP/LanL2DZ optimized structures of (a) NO_2/BNNS, (b) NO_2/C_B–BNNS, (c) NO_2/C_N–BNNS, (d) NO_2/Si_B–BNNS, (e) NO_2/Si_N–BNNS, (f) NO_2/Ge_B–BNNS and (g) NO_2/Ge_N–BNNS. The adsorption distances are in Å.

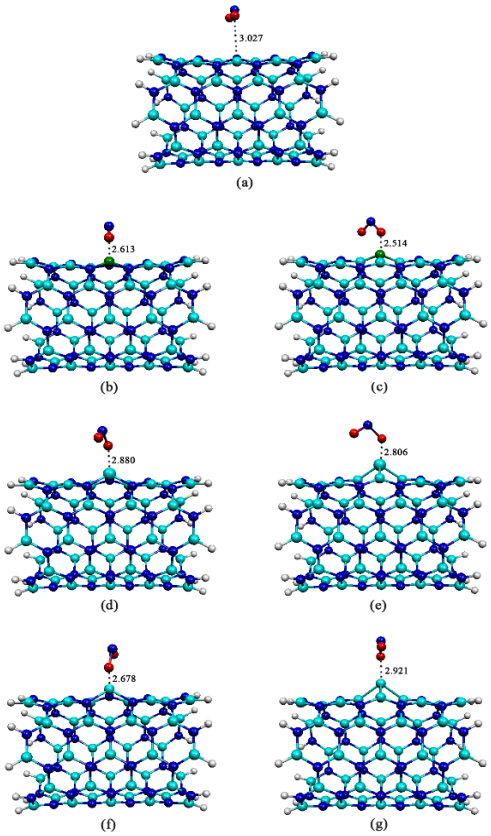

Figure 5 The B3LYP/LanL2DZ optimized structures of (a) NO_2/BNNT, (b) NO_2/C_B–BNNT, (c) NO_2/C_N–BNNT, (d) NO_2/Si_B–BNNT, (e) NO_2/Si_N–BNNT, (f) NO_2/Ge_B–BNNT and (g) NO_2/Ge_N–BNNT. The adsorption distances are in Å.

Table 3 Adsorption energies (E_{ads}), adsorption distances (ADs), energy gaps (E_g), and partial charge transfers (PCT) of NO_2 adsorbed on pristine, C–, Si–, and Ge–doped BNNS and BNNT

Species	E_{ads}[a]	AD[b]	E_g[c]	PCT[d]
NO_2/BNNS (2)	–2.31	3.110	1.85	0.024
NO_2/C_B–BNNS (1)	–48.57	2.296	3.37	–0.726
NO_2/C_N–BNNS (1)	–33.88	1.581	3.70	–0.270
NO_2/Si_B–BNNS (1)	–78.62	1.791	3.59	–0.606
NO_2/Si_N–BNNS (1)	–63.48	1.808	3.81	–0.548
NO_2/Ge_B–BNNS (1)	–67.17	1.881	3.54	–0.594
NO_2/Ge_N–BNNS (1)	–58.51	1.901	3.76	–0.545
NO_2/BNNT (2)	–3.52	3.027	1.28	0.022
NO_2/C_B–BNNT (1)	–52.30	2.613	3.92	–0.357
NO_2/C_N–BNNT (1)	–46.95	2.514	3.73	–0.251
NO_2/Si_B–BNNT (1)	–69.38	2.880	3.59	–0.563
NO_2/Si_N–BNNT (1)	–64.33	2.806	3.86	–0.545
NO_2/Ge_B–BNNT (1)	–47.45	2.678	2.78	–0.522
NO_2/Ge_N–BNNT (1)	–57.90	2.921	3.81	–0.544

[a] Spin multiplicities are in parenthesis.
[b] In kcal/mol.
[c] In Å.
[d] In eV.
[e] In e.

The PCTs between NO_2 molecule with pristine BNNS and BNNT are 0.024 and 0.022 e, respectively. The small PCT values occurred during NO_2 adsorption on pristine BNNS and BNNT confirm a weak interaction between the BNNS and BNNT with NO_2 molecule. The PCTs between the NO_2 and AT doped–BNNS and BNNT are found in the range of –0.726 to –0.270 and –0.565 to –0.251 e, respectively. the PCT analysis indicates that partial charges are transferred from C–, Si–, or Ge–doped BNNS and BNNT to the NO_2 molecule. In addition, the PCTs of NO_2 adsorption on AT doped–BNNS and BNNT are found to be larger than that of the pristine BNNS and BNNT. This supports that the doping of C, Si, and Ge atom on BNNS and BNNT affects in the electronic properties of the pristine BNNS and BNNT after adsorption.

4. Conclusions

The adsorption of NO_2 molecule adsorbed on the pristine and C–, Si–, and Ge–doped BNNSs and BNNTs at B or N sites were investigated using the DFT method. The binding energies of doped–BBNSs and BNNTs are found in the range of –103.50 to –332.63 and –118.67 to –320.44 kcal/mol, respectively. The binding energies reveal that the C atom doping exhibits the strongest binding ability with BNNS and BNNT. The AT doped–BNNSs and BNNTs display higher adsorption strength to NO_2 molecule than the pristine BNNS and BNNT. The significant increase in adsorption energy and charge transfer is probable to induce significant changes in the electrical conductivity of the AT doped–BNNS and BNNT. Therefore, C–, Si–, and Ge–doped BNNS and BNNT cab be used as advancing material for reliable and efficient NO_2 storage and sensing.

Acknowledgements

The financial support (2562A14702007) by Research and Development Institute, Rajabhat Maha Sarakham University is gratefully acknowledged. We also thank the Computational Chemistry Center for Nanotechnology (CCCN), Department of Chemistry, Faculty of Science and Technology, Rajabhat Maha Sarakham University, and Center of Excellence for Innovation in Chemistry (PERCH–CIC), Department of Chemistry, Faculty of Science, Mahasarakham University for the facilities provided.

Declaration of conflicting interests

The authors declared that they have no conflicts of interest in the research, authorship, and this article's publication.

References

1. Chopra N.G., Luyken R.J., Cherrey K., Crespi V.H., Cohen M.L., Louie S.G., and Zettl A. Boron nitride nanotubes. Science. 1995. 269 : 966–967.

2. Novoselov K.S., Jiang D., Schedin F., Booth T.J., Khotkevich V.V., Morozov S.V., and Geim A.K. Two–dimensional atomic crystals. Proc. Natl. Acad. Sci. USA. 2005. 102 : 10451–10453
3. Golberg D., Bando Y., Huang Y., Terao T., Mitome M., Tang C., and Zhi C. Boron Nitride Nanotubes and Nanosheets. Acs Nano. 2010. 4 : 2979–2993.
4. Yazyev O.V. and Pasquarello A. Metal adatoms on graphene and hexagonal boron nitride: towards rational design of self–assembly templates. Phys. Rev. B. 2010. 82 : 045407 – 045412.
5. Noorizadeh S. and Shakerzadeh E. Formaldehyde adsorption on pristine, Al–doped and mono–vacancy defected boron nitride nanosheets: A first principles study. Comput. Mater. Sci. 2012. 56 : 122–130.
6. Phalinyot S., Tabtimsai C., and Wanno B. Nitrogen monoxide storage and sensing applications of transition metal–doped boron nitride nanotubes: a DFT investigation. Struct. Chem. 2019. 30 : 2135–2149.
7. Xie Y., Huo Y–P., and Zhang J–M. First–principles study of CO and NO adsorption on transition metals doped (8,0) boron nitride nanotube. Appl. Surf. Sci. 2012. 258 : 6391–6397.
8. Sripadung P., Nunthaboot N., and Wanno B. DFT investigation of O_2 and PH_3 adsorptions on group 8B metal–doped boron nitride nanotubes. Sci. & Tech. RMUTT J. 2018. 8(2) : 53–64.
9. Venkataramanan N.S., Khazaei M., Sahara R., Mizuseki H., and Kawazoe Y. First–principles study of hydrogen storage over Ni and Rh doped BN sheets. Chem. Phys. 2009. 359 : 173–178.
10. Sripadung P., Nunthaboot N., and Wanno B. Group 8B transition metal-doped (5,5) boron nitride nanotubes for NH_3 storage and sensing: a theoretical investigation. Monatsh. Chem. 2019. 150 : 1011–1018.
11. Behmagham F., Vessally E., Massoumi B., Hosseinian A., and Edjlali L. A computational study on the SO_2 adsorption by the pristine, Al, and Si doped BN nanosheets. Superlattice. Microst. 2016. 100 : 350–357.
12. Deng Z–Y., Zhang J–M., and Xu K–W. First–principles study of SO_2 molecule adsorption on the pristine and Mn–doped boron nitride nanotubes. Appl. Surf. Sci. 2015. 347 : 485–490.
13. Al–Sunaidi A. Adsorption of SO_2 and NO_2 on metal–doped boron nitride nanotubes: A computational study. Comput. Theor. Chem. 2016. 1092 : 108–113.
14. Vanalakar S.A., Patil V.L., Harale N.S., Vanalakar S.A., Gang M.G., Kim J.Y., Patil P.S., and Kim J.H. Controlled growth of ZnO nanorod arrays via wet chemical route for NO_2 gas sensor applications, Sens. Actuators B. 2015. 221 : 1195–1201.
15. Lamsal L.N., Martin R.V., van Donkelaar A., Steinbacher M., Celarier E.A, Bucsela E., Dunlea E.J., and Pinto J. P. Ground–level nitrogen dioxide concentrations inferred from the satellite–borne ozone monitoring instrument. J. Geophys. Res. 2008. D16308. 113 : 1–15.
16. Kim J.S., Yoon J.W., Hong Y.J., Kang Y.C., Abdel–Hady F., Wazzan A.A., and Lee J.H. Highly sensitive and selective detection of ppb–level NO_2 using multi–shelled WO_3 yolk–shell spheres. Sens. Actuators B. 2016. 229 : 561–569.
17. Frisch M.J., Trucks G.W., Schlegel H.B., Scuseria G.E., Robb M.A., Cheeseman J.R., Montgomery J.A., Vreven T., Kudin K.N., Burant J.C., Millam J.M., Lyengar S. S., Tomasi J., Barone V., Mennucci B., Cossi M., Scalmani G., Rega N., Petersson G.A., Nakatsuji H., Hada M., Ehara M., Toyota K., Fukuda R., Hasegawa J., Ishida M., Nakajima T., Honda Y., Kitao O., Nakai H., Klene M., Li X., Knox J.E., Hratchian H.P., Cross J. B., Adamo C., Jaramillo J., Gomperts R., Stratmann R.E., Yazyev O., Austin A., Cammi R., Pomell C., Ochterski J. W., Ayala P.Y., Morokuma K., Voth G.A., Salvador P., Dannenberg J.J., Zakrzewski V G., Dapprich S., Daniels A. D., Strain M.C., Farkas O., Malick D.K., Rabuck A.D., Raghavachari K., Foresman J.B., Ortiz J., Cui Q., Baboul A.G., Clifford S., Cioslowski J., Stefanov B.B., Liu G., Liashenko A., Piskorz P., Komaromi I., Martin R.L., Fox D.J., Keith T., Laham M.A., Peng C.Y., Nanayakkara A., Challacombe M., Gill P.M., Johnson B., Chen W., Wong M.W., Gonzalez C., and Pople J.A, GAUSSIAN 09. Revision A.02, Gaussian Inc., Wallingford, CT, 2009.
18. Lee C., Yang W., and Parr R.G. Development of the Colle–Salvetti correlation–energy formula into a functional of the electron density. Phys. Rev. B. 1988. 37 : 785–789.
19. Becke A.D. Density–functional thermochemistry. III The role of exact exchange. J. Chem. Phys. 1993. 98 : 5648–5652.
20. Becke A.D. Density–functional exchange–energy approximation with correct asymptotic behavior. Phys. Rev. A. 1988. 38 : 3098–3100.
21. Hay P.J. and Wadt W.R. *Ab initio* effective core potentials for molecular calculations. Potentials for the transition metal atoms Sc to Hg. J. Chem. Phys. 1985. 82 : 270–283.
22. Hay P.J. and Wadt W.R. *Ab initio* effective core potentials for molecular calculations. Potentials for main group elements Na to Bi J. Chem. Phys. 1985. 82 : 284–298.
23. Hay P.J. and Wadt W.R. Initio effective core potentials for molecular calculations. Potentials for K to Au including the outermost core orbital. J. Chem. Phys. 1985. 82 : 299–310.
24. Baei M.T, Bagheri Z., and Peyghan A.A. Transition metal atom adsorptions on a boron nitride nanocage. Struct. Chem. 2013. 24 : 1039–1044.

25. Kaewruksa B. and Ruangpornvisuti V. Theoretical study on the adsorption behaviors of H_2O and NH_3 on hydrogen–terminated ZnO nanoclusters and ZnO graphene–like nanosheets. J. Mol. Struct. 2011. 994 : 276–282.
26. Vessally E., Dehbandi B., and Edjlali L. DFT study on the structural and electronic properties of Pt–doped boron nitride nanotubes. Russ. J. Phys. Chem. A. 2016. 90 : 1217– 1223.
27. Foster J.P. and Weinhold F. Natural hybrid orbitals natural hybrid orbitals. J. Am. Chem. Soc. 1980. 102(24) : 7211–7218.
28. Flükiger P., Lüthi H.P., and Portmann S. MOLEKEL 4.3. Swiss Center for Scientific Computing, Manno, Switzerland, 2000.
29. Almen N., Erni R., Kisielowski C., Rossell M.D., Gannett W., and Zettl A. Automically thin hexagonal boron nitride probed by ultrahigh-resolution transmission electron microscopy. Phys. Rev. B. 2009. 80 : 155425–155431.
30. Noorizadeh S. and Shakerzadeh E. Formaldehyde adsorption on pristine, Al-doped and mono-vacancy defected boron nitride nanosheets: A first principles study. Comput. Mater. Sci. 2012. 56 : 122–130.
31. Tabtimsai C., Nonsri A., Gratoo N., Massiri N., Suvanvapee P., and Wanno B. Carbon monoxide adsorption on carbon atom doped perfect and Stone–Wales defect single-walled boron nitride nanotubes: A DFT investigation. Monatsh. Chem. 2014. 145 : 725–735.
32. Peyghan A.A., Baei M.T., Moghimi M., and Hashemian S. Phenol adsorption study on pristine, Ga-, and In-doped (4,4) armchair single-walled boron nitride nanotubes. Comput. Theor.Chem. 2012. 997 : 63–69.
33. Oku T. and Narita I. Atomic structures and stabilities of zigzag and armchair-type boron nitride nanotubes studied by high-resolution electron microscopy and molecular mechanics calculation. Diamond Relat. Mater. 2004. 13:1254–1260.